Visual Terrain Estimation For Legged Robots

Frederike Dümbgen

July 27, 2016

Contents

Chapter 1

Introduction

1.1 Motivation

Why do Dense SLAM with B-Splines?

Overview of Dense SLAM algorithms in literature. Overview of Stereo Reconstruction algorithms. Overview of B-Splines usages in literature.

Goal of the project

1.2 Overview

Summary of the contents of this report.

Chapter 2

Methods

2.1 General

2.1.1 Coordinate Systems

Camera poses described by $_M\boldsymbol{r}_{MC_k}$ and $\boldsymbol{C}_{C_kM}$ for $k = 1, 2$ or

$$\boldsymbol{\xi}_{C_k} := \left[_M\boldsymbol{r}_{MC_k}, \boldsymbol{\Phi}_{C_kM}\right]^T$$
$$\boldsymbol{\xi}_S := \left[_M\boldsymbol{r}_{MS}, \boldsymbol{\Phi}_{SM}\right]^T$$

with $\boldsymbol{\Phi}_{C_kM}$, $\boldsymbol{\Phi}_{SM} \in \mathbb{R}^3$ [1]

How are the coordinate systems defined and related w.r.t each other?

2.1.2 Camera Projections

How to obtain the pixel coordinates from map points and jacobians.

$$\boldsymbol{u}_{j,k} = \boldsymbol{K}_k D_k(\boldsymbol{T}_k(_M\boldsymbol{r}_{MX_j}))$$
$$\boldsymbol{T}_k(_M\boldsymbol{r}_{MX_j}) = \boldsymbol{\pi}(\boldsymbol{C}_{C_kM}(_M\boldsymbol{r}_{MX_j} - _M\boldsymbol{r}_{MC_k}))$$

with I_1, I_2 interpolated intensities

$$_M\boldsymbol{r}_{MX_j} = \left[x_j, y_j, h(x_j, y_j)(\boldsymbol{a})\right]^T$$

2.1.3 Interpolations

Splines

Interpolations used for splines calculation

$$h(x_j) = \sum_{i=0}^{M} a_i h_i(x_j)$$

$$= \sum_{i=k}^{k+s} a_i h_i(x_j), \text{ for } j = 1 \dots N$$

Image interpolation

Interpolation used to interpolate between pixels

2.2   Mapping

2.2.1   Photometric Error Calculation

Photometric error of grid point x_j, y_j:

$$r_j(\boldsymbol{a}) = I_1(\boldsymbol{u}_{1,j}(\boldsymbol{a})) - I_2(\boldsymbol{u}_{2,j}(\boldsymbol{a})) \ ,$$

2.2.2   Optimization Setup

$$\hat{\boldsymbol{a}} = \arg\min_{\boldsymbol{a}\in\mathbb{R}^M} f(\boldsymbol{a}) = \arg\min_{\boldsymbol{a}\in\mathbb{R}^M} \frac{1}{2}(\sum_{j=0}^{N} w_j r_j(\boldsymbol{a})^2 + \beta\boldsymbol{a}^T\boldsymbol{B}\boldsymbol{a} + \gamma\boldsymbol{a}^T\boldsymbol{G}\boldsymbol{a}) \ ,$$

$$\boldsymbol{J}_r(\boldsymbol{a}) = \frac{\partial\boldsymbol{r}(\boldsymbol{a})}{\partial\boldsymbol{a}} \in \mathbb{R}^{N\times M}$$

2.2.3   Solver Scheme

$$\boldsymbol{a}_{k+1} = \boldsymbol{a}_k + \boldsymbol{p}_k^{GN}$$
$$\boldsymbol{J}_r(\boldsymbol{a})^T\boldsymbol{J}_r(\boldsymbol{a})\boldsymbol{p}_k^{GN} = -\ \boldsymbol{J}_r(\boldsymbol{a})^T\mathbf{r}(\boldsymbol{a})$$

2.3   Localization

2.3.1   Photometric Error Calculation

$$r_{1,j}(\boldsymbol{\xi}) = I_1(\boldsymbol{u}_{1,j}(\boldsymbol{\xi})) - \hat{I}(x_j, y_j)$$
$$r_{2,j}(\boldsymbol{\xi}) = I_2(\boldsymbol{u}_{2,j}(\boldsymbol{\xi})) - \hat{I}(x_j, y_j)$$

$$\boldsymbol{J}_r(\boldsymbol{\xi}) = \frac{\partial\boldsymbol{r}(\boldsymbol{\xi})}{\partial\boldsymbol{\xi}} \in \mathbb{R}^{N\times 6}$$

2.3.2   Optimization Setup

$$\hat{\boldsymbol{\xi}} = \underset{\hat{\boldsymbol{\xi}} \in \mathbb{R}^6}{\arg\min} \; \frac{1}{2} \sum_{j=0}^{N} r_j(\boldsymbol{\xi})^2$$

2.3.3   Solver Scheme

$$\boldsymbol{\xi}_{k+1} = \boldsymbol{\xi}_k \boxplus \mathbf{p}_k^{GN}$$
$$\boldsymbol{J}_r(\boldsymbol{\xi})^T \boldsymbol{J}_r(\boldsymbol{\xi}) \mathbf{p}_k^{GN} = - \, \boldsymbol{J}_r(\boldsymbol{\xi})^T \mathbf{r}_k(\boldsymbol{\xi})$$

Chapter 3

Results

Chapter 4

Conclusion

4.1 Achievements

4.2 Future Work

Appendices

Appendix A

Parameters

A.1 Rectification Test

The following test was performed to verify the correctness of the pixel associations with respect to the rectified images given by *image_proc* of `ROS`. The difference of intensities at corresponding pixels in the original images I_j and rectified images I_j^{rect} are given by:

$$\Delta I_{i,j} = I_j(u_{i,j}) - I_j^{rect}(w_{i,j}) \quad \text{for } i = 1 \dots n, \quad j = 1, 2 \quad , \tag{A.1}$$

where $u_{i,j}$, $w_{i,j}$ denote the pixel location of the object point X_i in the original and rectified image of camera j respectively.

If the rectified pixels are computed in accordance with the rectification process given by `ROS`, this difference should be approximately zero or

$$I_j(u_{i,j}) = I_j^{rect}(w_{i,j}) + \epsilon_{i,j} \quad \text{for } i = 1 \dots n, \quad j = 1, 2 \quad , \tag{A.2}$$

with the error $\epsilon_{i,j}$ arising solely from interpolation.

The pixels of the rectified images are computed using the projection matrices $P_j = K' \left[I | t_j \right]$ and rotation matrices R_j obtained from the *CameraInfo* message with [**?**]

$$w_{i,j} = K'(R_j T_j(X_i)) \quad , \text{where} \tag{A.3}$$
$$T_j(X_i) = \pi(_{C_j} r_{C_j X_i}) \tag{A.4}$$
$$= \pi(C_{C_j M}(X_i - {}_M r_{MC_j})) \quad \text{and} \tag{A.5}$$
$$\pi((x, y, z)^T) = (x/z, y/z, 1)^T \quad . \tag{A.6}$$

The parameters related to the pose of each camera are obtained from

$$C_{C_jM} = C_{C_jS}C_{SM} = R_j^T C_{SM} \quad \text{and} \tag{A.7}$$

$$_M r_{MC_j} = C_{MS}(_S r_{SC_j} -_S r_{SM}) \tag{A.8}$$

$$= C_{MS}(-t_j -_S r_{SCM}) \quad . \tag{A.9}$$

The pose of the stereo frame with respect to the map frame $(C_{MS},\ _M r_{MS})$ is estimated such that all map point projections lie inside both images.

The last information missing for calculating the pixel correspondences are the distorted pixels which are simply given by

$$u_{i,j} = K_j D_j(T_j(X_i))) \quad \text{for } i = 1 \dots n, \quad j = 1, 2 \quad , \tag{A.10}$$

with K_j and D_j the camera matrix and distortion function and T_j the same projection function as given above.

A look at Figures A.1a and A.1b shows that the resulting error between the rectified image and the original image is indeed uniformly small and with only very light patterns observable in both left and right images. These patterns get stronger as we approach the image border, where interpolation effects become more important. The pixel correspondence equations developed above are thereby validated for the rectified images provided by *image_proc*.

A.2 Transformation Test

Similar considerations can be applied for validating the interpretation of the camera parameters to compute the transformation between the left and the right camera.

The following assumptions need to be tested [**?**], [**?**, p. 523f].

$$C_{SC_j} = R_j \quad \text{and} \quad {}_S r_{SC_j} = -t_j \quad \text{for j=1,2} \quad . \tag{A.11}$$

If the above assumptions hold, then one can obtain the point coordinates in the second camera frame from the ones in the first camera frame by applying

$$_{C_2} r_{C_2 X_i} = C_{C_2 C_1}({}_{C_1} r_{C_1 X_i} + {}_{C_1} r_{C_1 C_2}) \quad \text{for } i = 1 \ldots n, \text{with} \tag{A.12}$$

$$C_{C_2 C_1} = R_2^T R_1 \quad \text{and} \tag{A.13}$$

$$_{C_1} r_{C_1 C_2} = C_{C_1 S}({}_S r_{SC_2} - {}_S r_{SC_1}) \tag{A.14}$$

$$= R_1^T(t_1 - t_2) \quad . \tag{A.15}$$

The same transformations as before are then applied to project these points in the respective rectified images.

As can be seen from Figure A.1c, the resulting intensity difference image is identical with the one from the preceding procedure where the pixels were directly projected from the world frame to the left and right image (Figure A.1b). Therefore, the transform between the left and right image is computed correctly. *No! This only tells me that I was consistent with my transformations and not that the transformations are indeed right. . . (Check with examples with correct depth information if the transformations are right.)*

The photometric error in the original and rectified image are is shown in Figures A.2a and A.2b. Since at this stage, no reliable depth information is available, low photometric errors cannot be expected, which explains the relatively high average value. However, we know that the photometric errors should be approximately the same in the rectified and non-rectified images. This behaviour is indeed observable, as shown by the difference image (Figure A.2c).
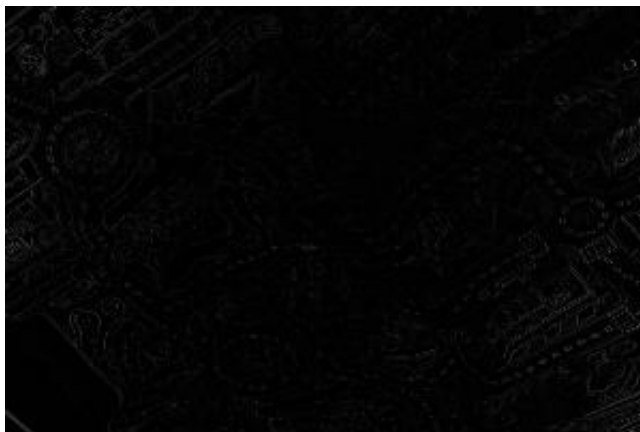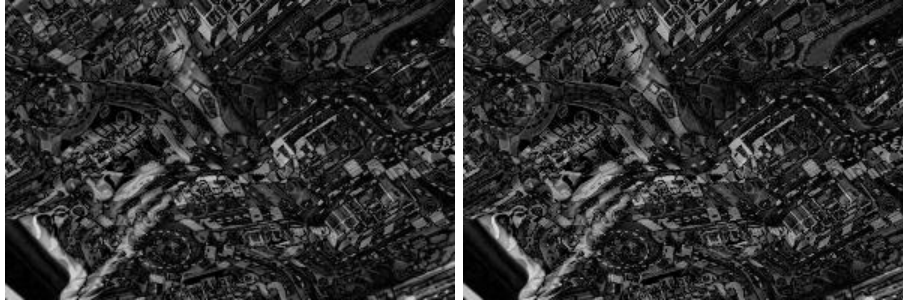
(a) Left image (mean: 4.78).
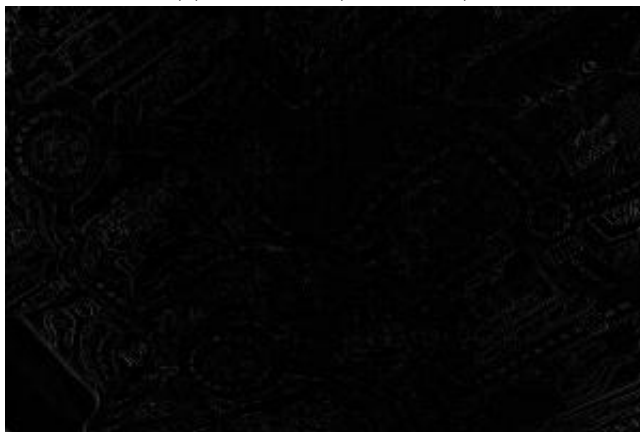
(b) Right image (mean: 4.34).

(c) Right image obtained with transformation (mean: 4.34).

Figure A.1: Rectification intensity errors $\Delta I_{i,j}$ with $n_x = 300$ and $n_y = 200$.

(a) Original image (mean: 44.97).

(b) Rectified image (mean: 46.23).

(c) Difference of original and rectified image (mean: 6.71).

Figure A.2: Rectification residual errors with $n_x = 300$ and $n_y = 200$.

Bibliography

[1] M. BLOESCH, H. SOMMER, T. LAIDLOW, M. BURRI, G. NUETZI, AND R. O. JUN, *A Primer on the Differential Calculus of 3D Orientations*, (2016).